GeoInformation in Europe, M.A. Gomarsca (ed.)


# Fuel type mapping from hyperspectral MIVIS and multispectral Landsat TM data in the fragmented ecosystems of southern Italy

R. Lasaponara, A. Lanorte
*Istituto di Metodologie per l'Analisi Ambientale, IMAA-CNR, C.da S.Loja – 85010 Tito Sc. (PZ), Italy, Tel.: ++39 0971 427 214; fax: ++39 0971 427 217*
*e-mail: lasaponara@imaa.cnr.it*

Keywords: fuel type, fire, satellite, MIVIS, TM

ABSTRACT: This paper is focused on the hyper- and multi-spectral characterization of fuel type at different spatial scales in the fragmented ecosystems of the Pollino National Park. To this aim, multisensor remote sensing acquired from hyperspectral Multispectral Infrared and Visible Imaging Spectrometer (MIVIS) and ASTER data were analysed for the test area. Fieldwork fuel type recognition, performed at the same time as remote sensing data acquisitions, were used to assess the results obtained for the considered test areas. Results from the classifications showed very satisfactory accuracy levels that were higher than 90% and 81% respectively for MIVIS. and ASTER data.

## 1 INTRODUCTION

In the context of fire management, fuel maps are essential information requested at many spatial and temporal scales for managing wildland fire hazard and risk and for understanding ecological relationships between wildland fire and landscape structure. Remote sensing data provide valuable information for the characterization and mapping of fuel types and vegetation properties at different temporal and spatial scales including the global, regional and landscape levels.

This study aims to ascertain how well remote sensing data can characterize fuel type at different spatial scales in fragmented ecosystems. For this purpose, multisensor and multiscale remote sensing data from the hyperspectral sensor named Multispectral Infrared and Visible Imaging Spectrometer (MIVIS) and ASTER data have been analysed for a test areas of Southern Italy characterized by mixed vegetation covers and complex topography. Two different approaches have been adopted for fuel type mapping: the well-established classification techniques and spectral mixture analysis. Fieldwork fuel type recognition, performed at the same time as remote sensing data acquisitions, was used to assess the results obtained for the considered test area.

Our investigations constitute a baseline for quantifying potential errors resulting from classification of lower spatial resolution images by using re-sampled classifications of higher spatial resolution data.

## 2 DATA AND STUDY AREAS

The selected study area extends over a territory of about 6,000 hectares inside the National Park of Pollino in the Basilicata Region (Southern Italy). It is characterized by complex topography with altitude varying from 400 m to 1900 m above sea level (asl) and mixed vegetation covers. Between 400 and 600 m natural vegetation is constituted by the Mediterranean scrubs, xeric prairies and Mediterranean shrubby formations. In the strip included between 600 and 1000–1200 m the characteristic vegetation is represented by poor populations of Quercus pubescens and from extensive woods of Turkey oaks (Quercus cerris); evident degradation forms are present, in the form of xerophytic prairies and substitution bushes. The higher horizons are constituted by beech woods (Fagus sylvatica) which arrive up to 1900 m: the deforested areas in this strip are generally engaged by mesophytic prairies used for pasture.

The remotely sensed characterization of fuel types was performed by adopting as reference the fuel types classification (Table 1) developed for Mediterranean ecosystems in the framework of the Prometheus project (Prometheus Project 1999).

Table 1. Fuel type classification developed for Mediterranean ecosystems in the framework of Prometheus project (Prometheus Project 1999).

| Fuel type class | Fuel type description in terms of percentage of cover | Fuel Type description in terms of vegetation typology |
|---|---|---|
| 1 | Ground fuels (cover > 50%) | grass |
| 2 | Surface fuels (shrub cover > 60%, tree cover < 50%) | grassland, shrub land (smaller than 0.3–0.6 m and with a high percentage of grassland), and clear cuts, where slash was not removed |
| 3 | Medium-height shrubs (shrub cover > 60%, tree cover < 50%) | shrubs between 0.6 and 2.0 m |
| 4 | Tall shrubs (shrub cover > 60%, tree cover < 50%) | high shrubs (between 2.0 and 4.0 m) and young trees resulting from natural regeneration or forestation |
| 5 | Tree stands (>4 m) with a clean ground surface (shrub cover < 30%) | the ground fuel was removed either by prescribed burning or by mechanical means. This situation may also occur in closed canopies in which the lack of sunlight inhibits the growth of surface vegetation |
| 6 | Tree stands (>4 m) with medium surface fuels (shrub cover > 30%) | the base of the canopies is well above the surface fuel layer (>0.5 m). The fuel consists essentially of small shrubs, grass, litter, and duff (the layer of decomposing organic materials lying immediately above the mineral soil but below the litter layer of freshly fallen twigs, needles, and leaves; the fermentation layer) |
| 7 | Tree stands (>4 m) with heavy surface fuels (shrub cover > 30%) | stands with a very dense surface fuel layer and with a very small vertical gap to the canopy base (<0.5 m) |

The hyperspectral data were acquired by the airborne MIVIS scanner (onboard a Spanish aircraft CASA 212) that is owned and managed by the Italian National Research Council in the context of LARA (Airborne Laboratory for Environmental Study) Project.

MIVIS acquired information in 102 spectral bands characterized by a non continuous spectral coverage between 0.4 μm and 12.7 μm. The survey was executed at an altitude of 4000 m a.s.l. (corresponding to a ground resolution varying from 7 m to 3.5 m with respect to altimeter variations) at a scan rate of 16.5 Hz. Additionally, air photos were acquired for the investigated region. Among the 102 MIVIS bands only the 28.

Channels in the Visible and Near InfraRed (VNIR) were considered, while the Thermal Infrared Region (TIR) (having a different ground resolution) and the Short Wave InfraRed (SWIR) channels were excluded because of the low signal-to-noise ratio due to solar irradiance in the autumn season.

ASTER is a high resolution imaging instrument that is flying on the Earth Observing System (EOS) Terra satellite. It has the highest spatial resolution of all five sensors on Terra and collects data in the visible/near infrared (VNIR), short wave infrared (SWIR), and thermal infrared bands (TIR). Each subsystem is pointable in the crosstrack direction. The VNIR subsystem of ASTER is quite unique. One telescope of the VNIR system is nadir looking and two are backward looking, allowing for the construction of 3-dimensional digital elevation models (DEM) due to the stereo capability of the different look angles. ASTER has a revisit period of 16 days, to any one location on the globe, with a revisit time at the equator of every four days. ASTER collects approximately eight minutes of data per orbit (rather than continuously).

Among the 14 ASTER bands (see Table 2) we only considered the 3 channels in the VNIR region and 6 channels in the SWIR region, while the TIR channels were excluded.

## 3 METHOD

In this study, the maximum likelihood classification (MLC) (Lillesand & Kiefer 2000) was adopted for fuel type mapping. This classification, as with other conventional hard classification techniques, assumes that all image pixels are pure. Nevertheless, this assumption is often untenable. In mixed land cover compositions, as pixels increase in

Table 2. MIVIS accuracy level.

| Class | Prod. Acc. (%) | User Acc. (%) |
|---|---|---|
| Fuel type 1 | 98.29 | 88.41 |
| Fuel type 2 | 89.20 | 71.71 |
| Fuel type 3 | 49.09 | 84.13 |
| Fuel type 4 | 96.24 | 73.04 |
| Fuel type 5 | 100.00 | 99.92 |
| Fuel type 6 | 95.44 | 99.52 |
| Fuel type 7 | 94.64 | 98.35 |
| No fuel | 99.14 | 98.68 |
| Unclassified | 99.38 | 100.00 |
| | Overall accuracy = 90.3964% | |
| | Kappa coefficient = 0.8905 | |

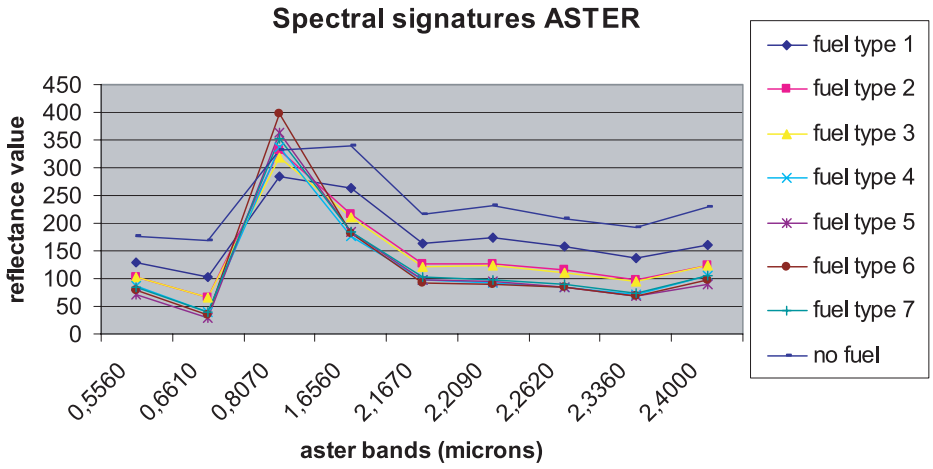


Figure 1. Spectral signatures obtained for the seven fuel types from ASTER data.

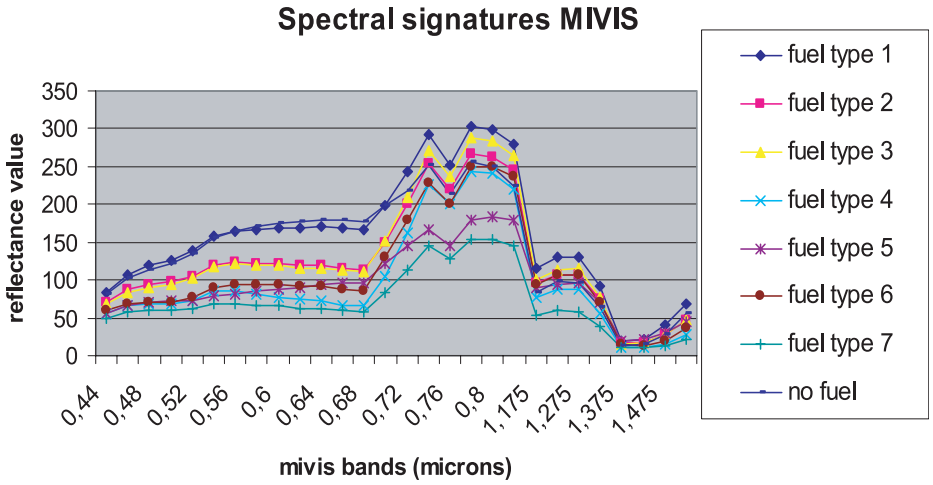


Figure 2. Spectral signatures obtained for the seven fuel types from MIVIS data.

size, the proportion of mixed cover type distributed at pixel level will likewise increase and information at the sub-pixel level will be of increasing interest. Consequently, in fragmented landscapes conventional "hard" image classification techniques provide only a poor basis for the characterization and mapping of fuel types giving, in the best case, a compromised accuracy, or, in the worst case, a totally incorrect classification.

In these conditions, the use of spectral mixture analysis (SMA) can reduce the uncertainty in hard classification techniques since it is able to capture, rather than ignore, subpixel heterogeneity. The SMA allows for classifying the proportions of the ground cover types (end-member classes) covered by each individual pixel. End-member classes

can be taken from "pure" pixels within an image or from spectral libraries. Over the years, different models of spectral mixtures have been proposed (Ichku & Karnieli 1996). Among the available models, the most widely used is the (Ichku & Karnieli 1996) Mixture Tuned Matched Filtering (MTMF) (that is based on the assumption that the spectrum measured by a sensor is a linear combination of the spectra of all components within the pixels.

On the basis of ground surveys and air photos, we selected the region of interest (ROI) corresponding to the considered 7 fuel types, plus 2 additional classes related to no fuel and unclassified regions. Results obtained from different remote data sources were compared on the basis of the achieved accuracy levels. Performance evaluation was performed adopting the following indices.

The producer's accuracy is a measure indicating the probability that the classifier has correctly labeled an image pixel, for example, into Fuel Type 1 class given that, on the basis of ground recognition such a pixel belongs to Fuel Type 1 class. The user's accuracy is a measure indicating the probability that a pixel belongs to a given class and the classifier has labeled the pixel correctly into the same given class. The overall accuracy is calculated by summing the number of pixels classified correctly and dividing by the total number of pixels. Finally, the kappa statistics (K) was also considered. It measures the increase in classification accuracy over that of pure chance by accounting for omission and commission error (Congalton & Green 1998). Overall accuracy is computed as the sum of the number of observations correctly classified (class1, as class 1, class 2 as class 2, etc.) divided by the total number of observations. This is equivalent to the "diagonal" of a square contingency table matrix divided by the total number of observations described in that contingency table.

Tables 2 and 3 only show the results from MLC obtained for MIVIS and ASTER data respectively, because the two classification approaches, MLC and MTMF, provided very close results, and no significant differences were found.

The producer's accuracy is a measure indicating the probability that the classifier has correctly labelled an image pixel, for example, into Fuel Type 1 class given that, on the basis of ground recognition such a pixel belongs to Fuel Type 1 class. The user's accuracy is a measure indicating the probability that a pixel belongs to a given class and the classifier has labelled the pixel correctly into the same given class. The overall accuracy is calculated by summing the number of pixels classified correctly and dividing by the total number of pixels. Finally, the kappa statistics (K) was also considered. It measures the increase in classification accuracy over that of pure chance by accounting for omission and commission error (Congalton & Green 1998). Overall accuracy is computed as the sum of the number of observations correctly classified (class1, as class 1, class 2 as class 2, etc.) divided by the total number of observations. This is equivalent to the "diagonal" of a square contingency table matrix divided by the total number of observations described in that contingency table (Congalton & Green 1998).

Table 2 shows that the confusion matrices resulting from the application of MLC to MIVIS data provided an overall accuracy of 90.4%, higher than the value (81.9%) obtained from ASTER images. The application of MTMF to ASTER MLC and MTMF, provided very close results, and no significant differences were found.

Table 3. ASTER accuracy level.

| Class | Prod. Acc. (%) | User Acc. (%) |
|---|---|---|
| Fuel type 1 | 93.95 | 88.91 |
| Fuel type 2 | 46.00 | 44.09 |
| Fuel type 3 | 59.13 | 77.71 |
| Fuel type 4 | 70.33 | 54.07 |
| Fuel type 5 | 95.70 | 88.58 |
| Fuel type 6 | 86.24 | 93.44 |
| Fuel type 7 | 82.39 | 82.95 |
| No fuel | 99.05 | 99.05 |
| Unclassified | 88.00 | 100.00 |
| | Overall accuracy = 81.9384% | |
| | Kappa coefficient = 0.7849 | |

As a whole, results from this analysis showed that, as expected, the use of airborne hyperspectral data allowed an increase in accuracy at around 8%. Such results clearly pointed out that the classification of both airborne hyperspectral and satellite ASTER can produce reasonably accurate mapping of fuel type. From both the classification methods adopted, MLC and MTMF, the accuracy level were higher than 89% and higher than 78% respectively for MIVIS and ASTER data. The current prices of ASTER imagery is significantly lower that those of airborne hyperspectral data. The main finding of our investigation clearly pointed out the advent of sensors, such as ASTER, with increased spatial resolution may improve the accuracy and reduce the cost of fuels mapping.

## 4 FINAL REMARKS

Airborne Hyperspectral MIVIS and satellite Advanced Spaceborne Thermal Emission and Reflection Radiometer (ASTER), have been processed for fuel type characterization and mapping. The analyses were performed by using two different classification approaches the MLC and MTMF. The fragmented ecosystems of Pollino national park was adopted as study case. Fieldwork fuel types recognitions, performed at the same time as remote sensing data acquisitions, were used as ground-truth dataset to assess the results obtained for the considered test areas. Results from both MIVIS and ASTER imagery substantially provide very satisfactory levels of accuracy. From both the classification methods adopted, MLC and MTMF, the accuracy level were higher than 89% and higher than 78% respectively for MIVIS and ASTER data.

## REFERENCES

Boardman, J.W., Kruse, F.A. & Green, R.O. 1995. Mapping target signatures via partial un-mixing of AVIRIS data. *Summaries of the Fifth JPL Airborne Geoscience Workshop, JPL Publication* 95-1: 23–26. NASA Jet Propulsion Lab., Pasadena, Calif.

Congalton, R.G., Green, K. 1998. Assessing the accuracy of remotely sensed data: principles and practices. Lewis Boca Raton.

Harsanyi, J.C., Chang, C. 1994. Hyperspectral image classification and dimensionality reduction: an orthogonal subspace projection approach. *IEEE Transations on Geoscience and Remote Sens*. 32: 779–785.

Ichku, C., Karnieli, A. 1996. A review of mixture modeling techniques for sub-pixel land cover estimation, *Remote Sensing Reviews* 13: 161–186.

Lillesand, T.M., Kiefer, R.W. 2000. *Remote sensing and image interpretation*. New York: Wiley.

Prometheus, S.V. Project. 1999. *Management techniques for optimisation of suppression and minimization of wildfire effects*. System Validation. European Commission. Contract number ENV4-CT98-0716.